nature catalysis

Article

https://doi.org/10.1038/s41929-024-01189-2

Electrocatalytic cyclic deracemization enabled by a chemically modified electrode

Received: 2 June 2023

Accepted: 10 June 2024

Published online: 11 July 2024

Check for updates

Cheng-Jie Zhu, Xiuying Yang & Jianchun Wang

Redox chemistry, which is frequently encountered in the formation of new bonds and stereocentres, relies on the compatibility of redox potentials. Despite recent advances, achieving a general electrocatalytic cyclic deracemization process without stoichiometric redox reagents remains a formidable challenge. Here we show that electrocatalytic cyclic deracemization of secondary alcohols can be accomplished through sequential iridium-catalysed enantioselective anodic dehydrogenation and rhodium-catalysed cathodic hydrogenation, utilizing metal hydride catalysis. A considerable hurdle arises as stronger hydride donors necessitate parent metal complexes to possess low reduction potentials, resulting in inherent redox potential incompatibility. Nonetheless, we overcame this incompatibility by leveraging a recyclable rhodium-catalyst-modified electrode as the cathode—an accomplishment that homogeneous rhodium catalysis could not achieve. Our approach enables chemoselective stereochemical editing of bioactive compounds with remarkable functional group tolerance. Surface characterization and mechanistic studies showcased the unique advantages conferred by the chemically modified electrode.

Contra-thermodynamic stereochemical editing presents a unique technique that decouples stereochemistry-defining steps from those governing connectivity formation[1]. Within this realm, deracemization emerges as an enticing yet uncommon technique, facilitating the selective conversion of a racemic mixture into a pure enantiomer without altering its chemical structure[2]. The obstacle for designing such a contra-thermodynamic process lies in the principle of microscopic reversibility[3]. Past attempts used chemical energy inputs to drive reactions out of equilibrium[4–11] but suffered from the need for stoichiometric redox reagents (Fig. 1a). Another daunting challenge in chemo-catalysis is the oxidation–reduction compatibility. Although various approaches have been employed to tackle this challenge, including spatiotemporal division strategies such as the one-pot two-step procedure[6] and the implementation of triphasic systems[7], their general applicability remains somewhat constrained. More recently, seminal works by Bach[12–19], Knowles and Miller[20] demonstrated that deracemization can be achieved by energy or electron transfer, combined with the touch of chiral catalysts. Remarkable recent advancements[21–27] further expand photochemical strategy, which now stand apart as a unique exception to the principle of microscopic reversibility, as forward and reverse reactions are able to traverse along different electronic surfaces[28].

Electrochemistry has emerged as a reliable synthetic tool for enabling mild and selective organic transformations[29–42]. It boasts a plethora of innate advantages, including the ease of scalability, the use of recyclable electrodes and the potential to achieve unparalleled chemoselectivity. Although electrochemistry's potential to push the boundary of deracemization has been contemplated[2], its realization remains elusive so far. We drew inspiration from enantioselective borrowing hydrogen catalysis, which has become a powerful approach that couples transfer hydrogenation with intermediate reaction (Fig. 1b)[43–45]. A fundamental criterion for this process is that the reactive intermediate should exhibit a higher propensity for accepting hydrides

Shenzhen Grubbs Institute and Department of Chemistry, Guangdong Provincial Key Laboratory of Catalysis, Southern University of Science and Technology, Shenzhen, China. e-mail: wangjc3@sustech.edu.cn

https://doi.org/10.1038/s41929-024-01189-2

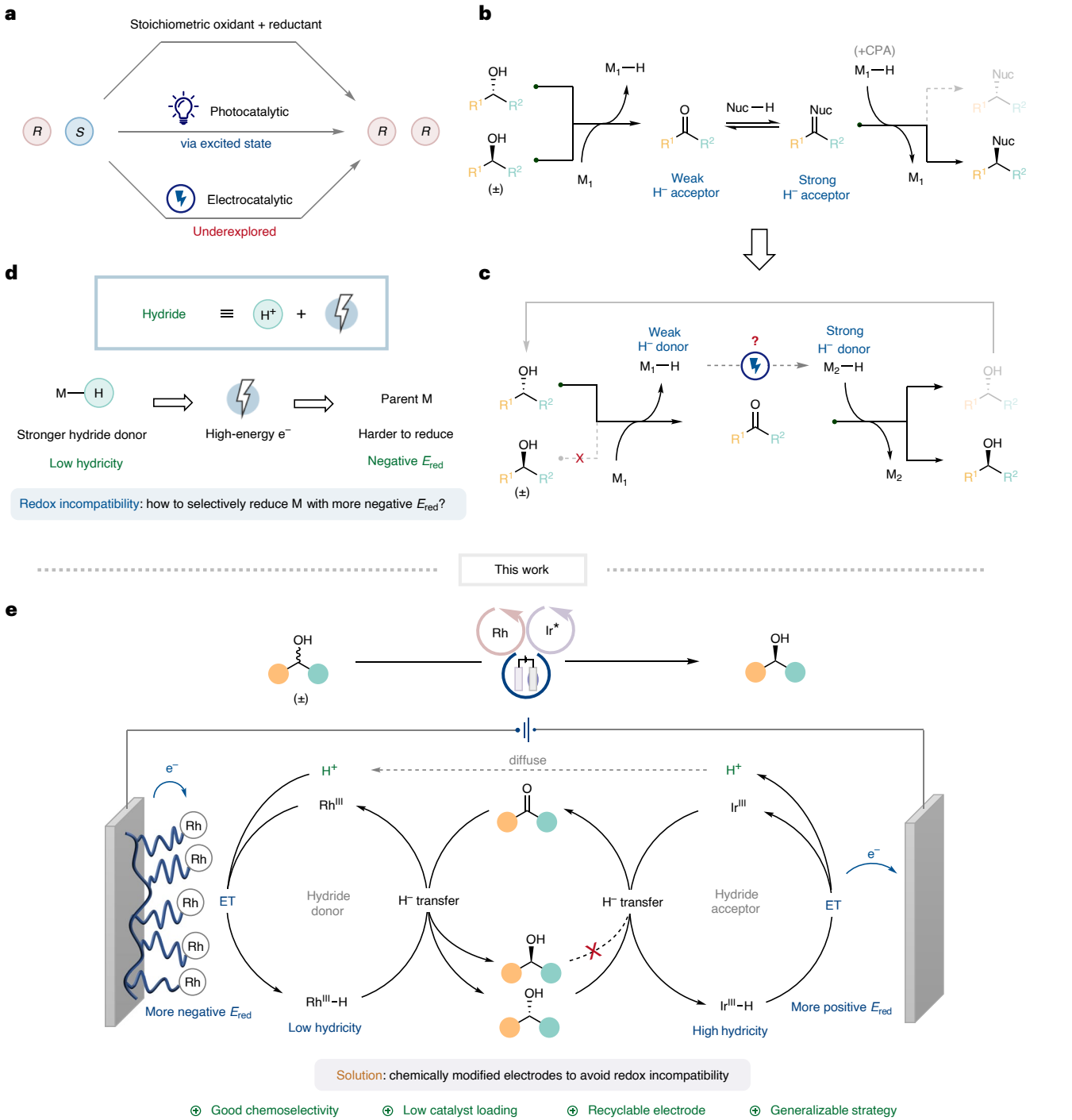

Fig. 1 | Electrocatalytic cyclic deracemization. a, Although chemically and photochemically driven deracemizations have been established, the electrocatalytic version has remained elusive. **b**, Enantioselective borrowing hydrogen catalysis necessitates the intermediate to be a stronger hydride acceptor than the original ketone. **c**, Electricity can be a driving force for converting a weak hydride into a potent one. **d**, Challenges for designing electrocatalytic cyclic deracemization. If the metal hydride acts as a stronger hydride donor, its parent metal must possess a more negative reduction potential. **e**, A CME was employed to tackle this inherent redox incompatibility.

compared with the original ketone[46–51]. Inspired by this, here we present a general strategy for achieving electrocatalytic cyclic deracemization (ECD) of secondary alcohols by employing a chemically modified electrode (CME) as the cathode. The input of electrical energy serves as the driving force, enabling the conversion of a weak hydride donor (M_1–H) into a potent one (M_2–H) (Fig. 1c). Here the physical separation of CME and the anode present a unique opportunity to bypass the principle of microscopic reversibility.

Results

Design plan

In this proof-of-concept study, deracemization of secondary alcohols is chosen as the model reaction. The process involves several key steps (Fig. 1c). First, the chiral catalyst M_1 selectively reacts with one enantiomer of the racemic alcohol to generate a ketone intermediate and M_1–H, which is subsequently oxidized at the anode, producing M_1 and H^+. Second, at the cathode, a different electrocatalyst M_2 needs to be

preferentially reduced and reacts with a proton to form M_2–H, which is a more potent hydride donor. Finally, the nascent M_2–H should convert the ketone intermediate back into the racemic alcohol, thus completing the catalytic cycle.

At first glance, this catalytic cycle seems to be a viable solution; however, upon closer scrutiny, it became evident that the requirements of hydricities and redox potentials were fundamentally at odds. A metal hydride can be formally considered as the addition of one proton and two electrons to the metal centre, meaning that higher-energy electrons (with more negative E_{red}) result in a more potent hydride donor (Fig. 1d). Indeed, Kubiak has demonstrated a strong correlation between hydricities and reduction potentials of parent metal complexes, regardless of the metal identities or ligand architectures[52]. In our case, it is necessary for M_2–H to be a more potent hydride donor than M_1–H, which implies that M_2 would have a more negative reduction potential than M_1. Conversely, for M_2 to be selectively reduced at the cathode, it must have a less negative reduction potential than M_1. To address this innate incompatibility, we devised a simple solution through the anchoring of M_1 onto the cathode to raise its local concentration, which prioritizes its reduction and prevents the re-oxidation of its reduced form (Fig. 1e). Although CME is a prominent approach within the energy conversion field to improve energy efficiency, its application in synthetic organic chemistry remains relatively uncommon[53–55]. Even rarer is the occurrence of immobilized heterogenous electrocatalysts exhibiting unusual reactivity compared with their homogeneous counterparts.

Reaction development

At the outset of this study, we sought to develop an efficient electrocatalytic oxidative kinetic resolution (OKR) method. Asymmetric transfer hydrogenation catalysts are renowned for their capacity to effectuate the OKR of secondary alcohols, using air or a sacrificial ketone as the terminal oxidant[56–60]. An electrochemical alcohol oxidation catalysed by an achiral iridium pincer complex in tandem with a phenoxy hydrogen atom transfer mediator was recently reported[61]. Unlike aerobic oxidation, the oxidation of transition metal hydrides through electricity typically unfolds in a stepwise process, involving sequential electron transfer and proton transfer, thus requiring a base for the electrocatalytic OKR[62,63]. With thorough catalyst screening and optimization of reaction conditions, we successfully achieved OKR of secondary alcohol **1** using Noyori–Ikariya-type catalysts (Fig. 2a). In accordance with past studies, the *N*-mesylated diamine iridium catalyst **Ir-1** proves superior to its counterpart, the *N*-tosylated catalyst **Ir-2**, as well as related rhodium and ruthenium catalysts (**Rh-1** and **Ru-1**). Weaker bases such as K_2CO_3 could also successfully promote the OKR approach (Supplementary Table 1). These experiments paved the way for the discovery of the ECD process.

Next, we aimed to choose an approach to immobilize an electrocatalyst that can effectively hydrogenate ketones. The well-established technique of pyrrole electropolymerization permits the deposition of an insoluble polymer directly on the electrode surface and offers easy control over the film thickness[64]. These polymer films also exhibit good chemical stability and possess a high concentration of active centres. As depicted in Fig. 2b, the anodic electropolymerization of **Rh-2** bearing a pedant *N*-substituted pyrrole could be successfully executed under anodic oxidation, yielding polymeric rhodium-catalyst-modified carbon felt electrodes (**Rh-CME**)[65]. Both the homogeneous $[Rh(dmbpy)_2Cl_2]PF_6$ (**Rh-3**, where dmbpy is 4,4′-dimethyl-2,2′-bipyridine) and the **Rh-CME** were able to catalyse electrocatalytic hydrogenation of **1′** successfully (Supplementary Table 3).

With those initial results in hand, we embarked on a quest to achieve ECD. To simplify the reaction set-up, we opted for constant current electrolysis method. After meticulous condition screening, successful ECD of model substrate *rac*-**1** could be accomplished with both high yield and enantioselectivity, using **Rh-CME** as the cathode (Fig. 2c, entry 1). We then conducted a series of control experiments to further understand the reaction. As anticipated, electricity was deemed a crucial factor for the reaction to proceed (entry 2 and Supplementary Table 2). The absence of rhodium catalysts resulted in the appearance of reductive pinacol coupling side products (entry 3), ruling out the possibility of ketones being hydrogenated by electrodes directly (Supplementary Fig. 12). Notably, when we replaced **Rh-CME** with the corresponding homogeneous catalyst **Rh-3**, only a meagre yield of (*S*)-**1** was obtained (entry 4). This finding aligns with our hypothesis and underscores the ability of modified electrodes to deliver novel reactivity, beyond merely improving efficiency. Carbon felt is superior to platinum foil as the anode material, as it probably prevents direct anodic oxidation of *rac*-**1** (entry 5)[66]. Similar results were obtained when a higher current was applied (entry 6), although this requires a slightly higher loading of rhodium. Vitamin E, which has been previously shown to effectively mediate hydrogen atom transfer from Ir–H species, proved detrimental in this ECD process (entry 7). Using acetonitrile as the solvent also decreased the yield (entry 8). The base itself served as the electrolyte, obviating the need for additional electrolytes (entry 9). A weaker base such as K_2CO_3 could also be used, albeit with reduced efficacy (entry 10). Using alternating current electrolysis also produced unsatisfactory outcomes (Supplementary Table 4).

Substrate scope

With the optimized conditions in hand, the substrate scope was then examined (Fig. 3). Broad functional group compatibility was observed with tolerance of fluoride (**7**, **14** and **15**), epoxide (**11**), Boc-protected amine (**12**), chloride (**16**), cyanide (**17**), acetal (**6** and **18**), thioether (**19**), trifluoromethyl (**20**) and ester (**48**). It is worth mentioning that K_2CO_3 could be employed as the base for substrates bearing hydrolysable functional groups. Interestingly, primary aliphatic alcohols (**10**) could be tolerated without being oxidized. This method was also compatible with medicinally interesting heterocycles such as furan (**21**), thiophene (**22**), pyrrole (**23**), quinoline (**25**) and pyridine (**47**). Both electron-rich (**6**, **10** and **11**) and poor (**7** and **8**) indanols are competent reactants, although highly electron-poor substrates were inclined to produce pinacol coupling side-products, probably through homocoupling of electrode-generated radical anions. This ECD method was applied to the deracemization of compound **26**, a synthetic intermediate towards a potent acid ceramidase inhibitor[67]. Six-membered rings such as 1-tetralol (**27** and **28**) and 4-chromanol (**29**) were also effective substrates. Diaryl alcohols such as 1-substituted fluorenol (**30**) underwent deracemization successfully. Our method can also be extended to the more challenging secondary aliphatic alcohols (**31**–**34**) with little steric difference. Notably, those aliphatic alcohols proved incompetent under Ikariya's aerobic OKR conditions (refer to Supplementary Figs. 15 and 16 for a detailed discussion). Furthermore, acyclic secondary alcohols can also be deracemized with success (**35**–**46**), although they tend to be less reactive. Heterocycles such as benzofuran (**36**) and benzothiophene (**37**) could be tolerated. When the alkyl group varied from methyl to a larger alkyl group (**46**), the reactivity diminished. Unfortunately, acyclic aliphatic secondary alcohols were unsuitable under current ECD conditions. To our delight, secondary alcohols derived from loratadine (**47**), menthol (**48**), ribofuranoside (**49**), perillyl alcohol (**50**), citronellol (**51**) and ospemifene (**52**) were deracemized successfully. Notably, 1,1-disubstituted olefin (**50**) was untouched even in the presence of Rh–H species.

Synthetic applications

One notable advantage of CMEs is their effortless separation from the reaction mixture, allowing for easy recycling. In our study, the **Rh-CME** exhibited remarkable reusability, as it could be rinsed with solvents and reused up to four times in the subsequent ECD reaction. This recycling process consistently afforded (*S*)-**1** in high yield and enantioselectivity (Fig. 4a). Note that it is believed that the Rh^I species

https://doi.org/10.1038/s41929-024-01189-2

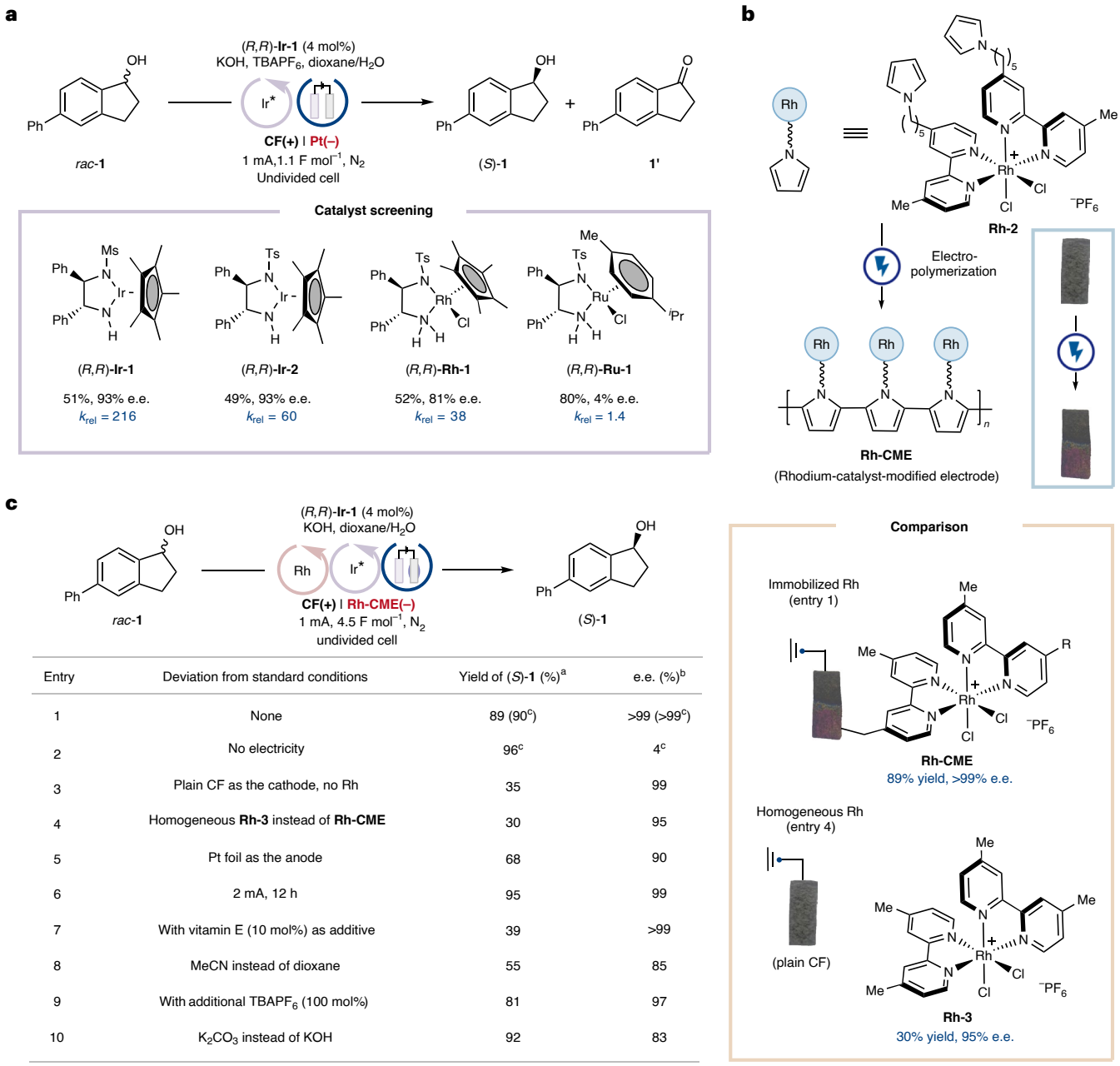

Entry	Deviation from standard conditions	Yield of (*S*)-**1** (%)[a]	e.e. (%)[b]
1	None	89 (90[c])	>99 (>99[c])
2	No electricity	96[c]	4[c]
3	Plain CF as the cathode, no Rh	35	99
4	Homogeneous **Rh-3** instead of **Rh-CME**	30	95
5	Pt foil as the anode	68	90
6	2 mA, 12 h	95	99
7	With vitamin E (10 mol%) as additive	39	>99
8	MeCN instead of dioxane	55	85
9	With additional $TBAPF_6$ (100 mol%)	81	97
10	K_2CO_3 instead of KOH	92	83

Fig. 2 | Reaction development. a, Initial investigation into an electrochemical iridium-catalysed oxidative kinetic resolution. Ms, mesyl; Ts, tosyl; CF, carbon felt; TBA, tetrabutylammonium. **b**, Preparation of a rhodium-catalyst-modified electrode by electropolymerization. **c**, Control experiments for electrocatalytic cyclic deracemization. [a]Yield determined by ^{1}H NMR using internal standard. [b]Enantiomeric excess (e.e.) values determined by ultra-performance convergence chromatography (UPCC). [c]Fully degassed 1,4-dioxane was used. $k_{rel} = \ln[(1-c)(1-\text{e.e.})]/\ln[(1-c)(1+\text{e.e.})]$, where c is conversion. See Supplementary Fig. 14 for experimental details.

form during the cathodic reaction, indicating the protective role of the polymer matrix for these otherwise vulnerable Rh^I species. Encouraged by the broad substrate scope, we explored application of this ECD method to late-stage stereochemical editing[68–70] of bio-active compounds. For instance, tetralol **53**, a non-steroidal progesterone receptor antagonist, holds promise in the treatment of gynaecological diseases[71]. Now, both (*R*)- and (*S*)-**53** could be accessed from deracemization of *rac*-**53** in a single step, which exemplifies the potential for rapid stereochemical editing of pharmaceutically relevant compounds (Fig. 4b). The substituted 3-cyclohexenol motif is a common feature in various bioactive compounds (Supplementary Fig. 17), yet achieving its enantioselective synthesis has proven challenging. Take, for example, the synthesis of (*R*)-**31**, which was recently accomplished through an elegant stereoselective [4+2]-cycloaddition process, requiring the use of a stoichiometric quantity of chiral alkenylborane **54** across a six-step procedure[72]. Remarkably, our ECD protocol now offers a direct pathway to access (*R*)-**31**, starting from the readily available *rac*-**31** (ref. 73) (Fig. 4c). Aside from the step economy and ease of derivatization, our method allows for the synthesis of both enantiomers. Interestingly, this ECD method also exhibited excellent chemoselectivity, selectively deracemizing the secondary alcohol in indenol moiety while leaving the acyclic secondary alcohol unaffected (**56**) (Fig. 4d). This ECD method could therefore represent a unique approach for accessing compounds with two configurationally distinct alcohol stereocentres, which could be challenging to synthesize from asymmetric hydrogenation of corresponding diketones. To illustrate, although classical CBS

https://doi.org/10.1038/s41929-024-01189-2

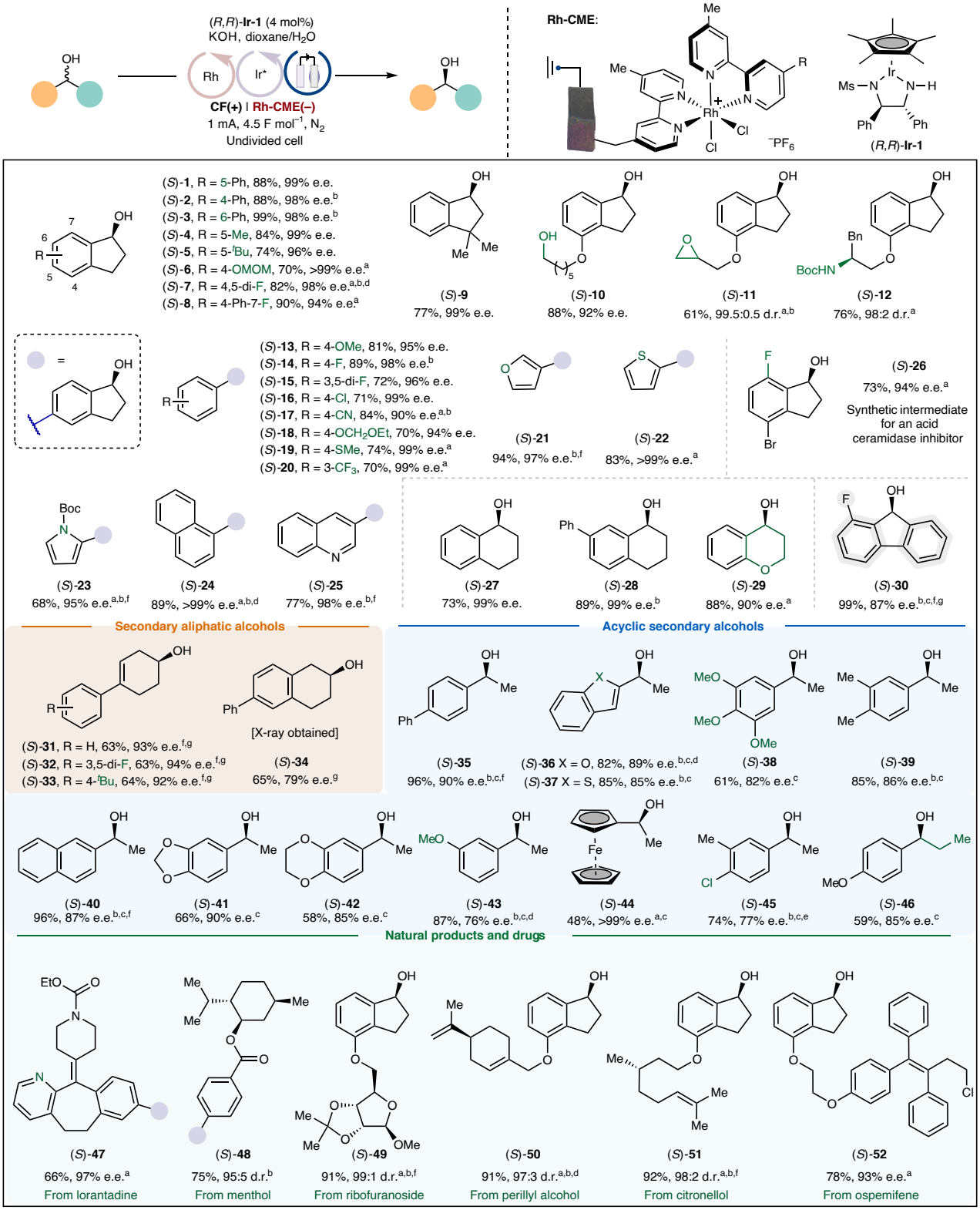

Fig. 3 | Substrate scope. Reaction conditions: secondary alcohols (0.2 mmol), (*R,R*)-**Ir-1** (4 mol%), KOH (0.2 mmol), 1,4-dioxane (2 ml) and H_2O (2 ml) at room temperature under a nitrogen atmosphere, in an undivided cell subject to 1 mA of current for 24 h using CF as the anode and **Rh-CME** as the cathode. The enantiomeric excess or diastereomeric ratio were determined via HPLC or UPCC analysis. [a]1,4-dioxane/2,2,2-trifluoroethanol/water (1:1:1) as solvent, K_2CO_3 (0.2 mmol) instead of KOH, nickel foam as the anode. [b]Subject to 2 mA of current. [c](*R,R*)-**Ir-1** (8 mol%). [d]At 35 °C. [e]At 40 °C. [f]At 45 °C. [g]Tetrahydrofuran and H_2O as solvent. Boc, *tert*-butyloxycarbonyl.

reduction can directly provide (*R,R*)-**57** and (*S,S*)-**57** from diketone **58**, obtaining (*S,R*)-**57** and (*R,S*)-**57** from diketone **58** poses greater difficulty (Fig. 4e). However, through selective epimerization[74–77] of the more reactive indanol moiety, (*S,R*)-**57** and (*R,S*)-**57** could be successfully delivered. Such a stereodivergent synthesis might hold relevance in the context of medicinal chemistry.

https://doi.org/10.1038/s41929-024-01189-2

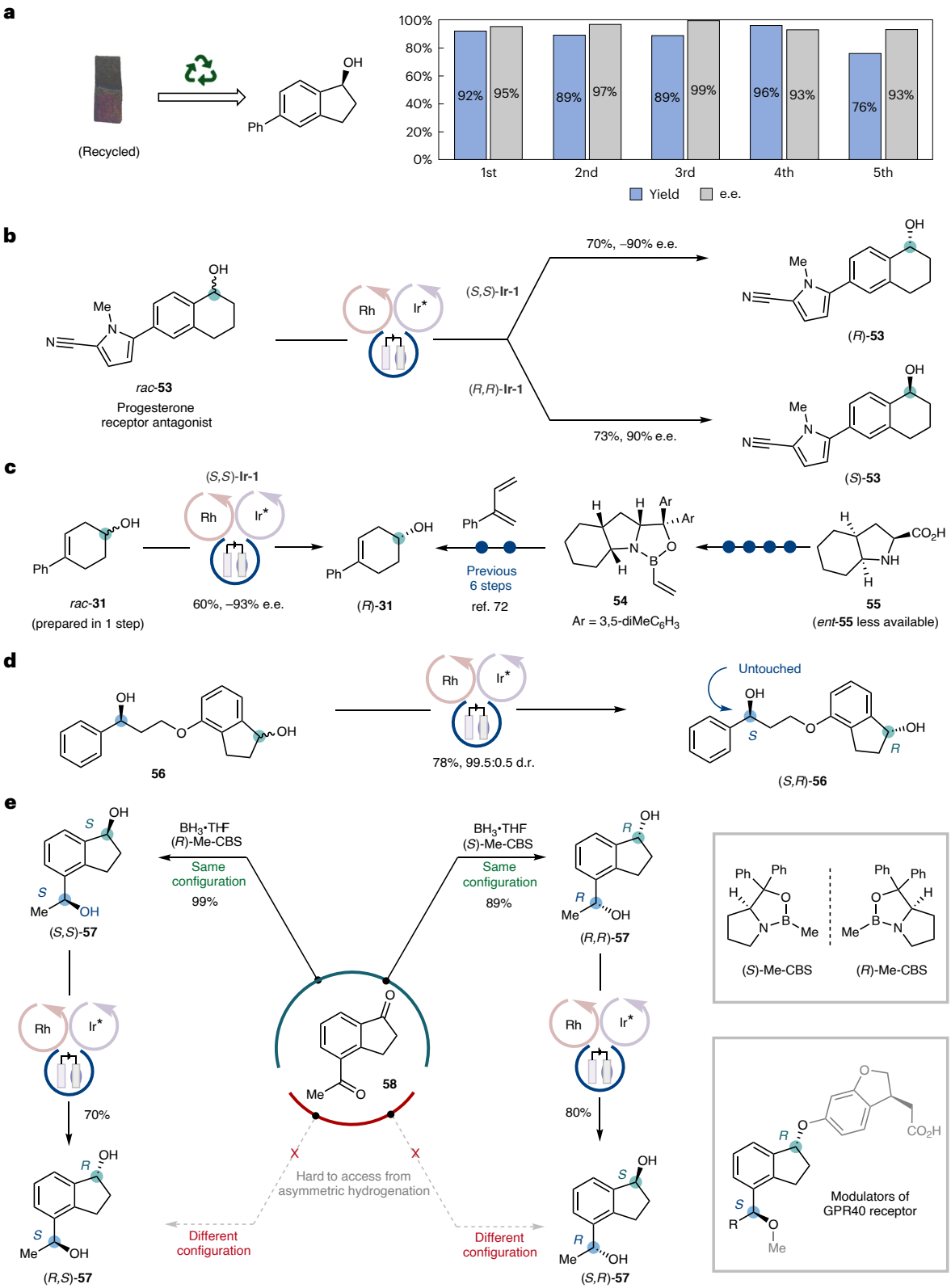

Fig. 4 | Synthetic applications. a, Chemically modified electrodes can be reused by rinsing them with solvents. **b**, Deracemization of a non-steroidal progesterone receptor. **c**, Expedited synthesis of substituted 3-cyclohexenol via ECD in comparison to the existing method. **d**, Selective deracemization of 1-indanol moiety while leaving the acyclic secondary alcohol untouched. **e**, Selective epimerization of the 1-indanol moiety can result in diols with stereocentres of different configurations, which can be challenging to access directly from asymmetric hydrogenation of diketones.

Mechanistic studies

We then conducted mechanistic studies to gain a deeper understanding. Our first objective was to provide evidence for the formation of metal hydrides through the combination of protons with electrons. A deuterium-labelling study using D_2O in lieu of H_2O afforded (*S*)-**59** with a ~52% deuterium ratio in both the α and β positions of the

https://doi.org/10.1038/s41929-024-01189-2

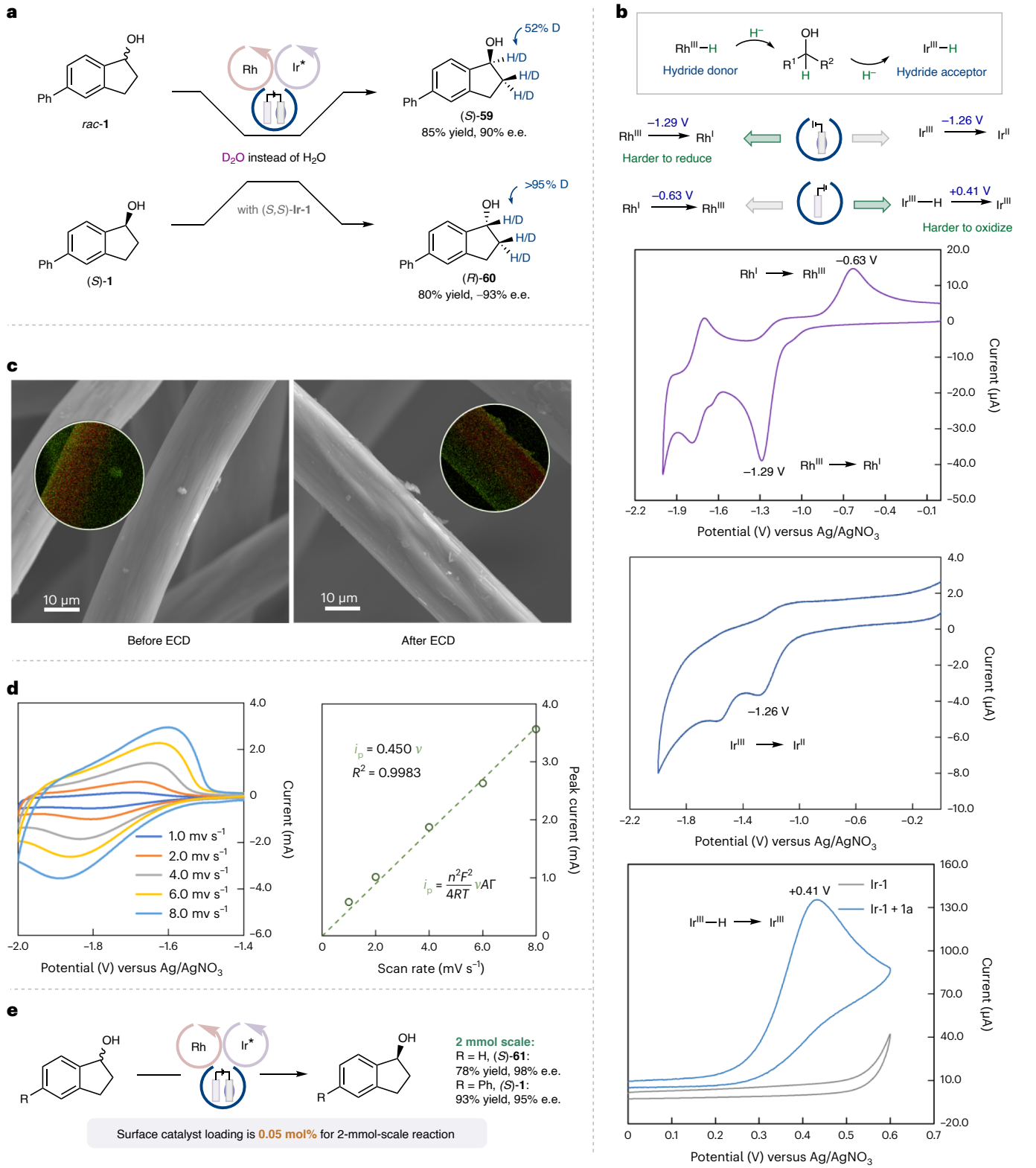

Fig. 5 | Mechanistic studies and characterization. a, Deuterium-labelling study. **b**, Cyclic voltammetric profiles of **Rh-2**, **Ir-1** and in situ-generated **Ir-1-H** in MeCN. **c**, SEM imaging of the modified electrode before and after ECD. The circled insets show EDS imaging. Green, rhodium; red, nitrogen; orange, fluorine. **d**, Left: scan rate dependence of **Rh-CME** in MeCN. Right: estimation of surface catalyst loading. $F = 96{,}485$ C mol^{-1}, n (number of electrons) = 1, $R = 8.314$ J K^{-1} mol^{-1}, $T = 298$ K, A = electrode surface area (cm^2), Γ = surface catalyst loading (mol cm^{-2}), peak current i_p (mA), scan rate υ (V s^{-1}). **e**, Surface catalyst loading could be decreased for larger-scale reactions.

alcohol, consistent with selective reaction with the (*R*)-configured isomer (Fig. 5a). When enantiopure substrate (*S*)-**1** was employed as the starting material, a >95% deuterium ratio was obtained in the enantiomerization product (*R*)-**60**. These results indicated that the Rh^{III}–H species probably came from electrochemical proton reduction instead of the unfavourable hydride transfer from the Ir^{III}–H species.

It is worth noting that our method also offers an interesting avenue for hydrogen isotope exchange using readily available deuterium oxide. We also monitored the reaction progress during the deracemization of *rac*-**1**, revealing the role of ketone **1′** as an intermediate (Supplementary Fig. 21).

Our investigations have revealed a crucial distinction between **Rh-CME** and homogeneous rhodium catalysts in the ECD process, highlighting the importance of redox potential compatibility. To verify our hypothesis experimentally, we first conducted cyclic voltammetry analysis on **Rh-2**, and observed an irreversible two-electron reduction process ($Rh^{III} \rightarrow Rh^{I}$, $E_p = -1.29$ V versus Ag/$AgNO_3$ 10 mM), followed by two reversible one-electron ligand-centred reduction processes[78] (Fig. 5b). The reverse scan showed an irreversible oxidation peak ($E_p = -0.63$ V), corresponding to the two-electron reoxidation of the metal centre ($Rh^{I} \rightarrow Rh^{III}$). Notably, under our basic conditions, the resting state of the rhodium catalyst should mostly be Rh^{I} rather than Rh^{III}–H species, given that the pK_a of $[Rh(bpy)_2(H_2O)H]^{2+}$ is 9.5 in water[79]. Regarding the iridium complex **Ir-1**, we observed an irreversible two-step metal-centred reduction process ($Ir^{III} \rightarrow Ir^{II}$, $E_p = -1.26$ V versus Ag/$AgNO_3$ 10 mM), which is slightly more facile than the reduction of **Rh-2** (−1.26 V versus −1.29 V) (Fig. 5b). Thus, the selective reduction of immobilized Rh^{III} in the presence of homogeneous Ir^{III} species can be attributed to the increased local concentration of Rh^{III} on the electrode surface. On the other hand, during the oxidative scan of in situ-generated iridium hydride **Ir-1-H**, an irreversible peak was observed, corresponding to the oxidation of the iridium hydride ($E_p = +0.41$ V). These cyclic voltammetry data demonstrated that Rh^{I} species should be more susceptible to oxidation than **Ir-1-H** (−0.63 V versus +0.41 V). The immobilized polymeric rhodium catalyst's inability to migrate to the anode effectively circumvents such redox incompatibility concerns (Supplementary Fig. 8). Furthermore, kinetic studies revealed that **Rh-3** and **Rh-CME** exhibited a comparable rate in the electrochemical hydrogenation of ketones, providing additional support for the notion that their disparities in the ECD process primarily stem from redox compatibility rather than differences in reactivity (Supplementary Fig. 9).

Surface characterization

The modified electrode surfaces were further characterized by scanning electron microscopy (SEM) imaging and energy-dispersive X-ray spectroscopy (EDS). Examination of a freshly prepared modified electrode (Fig. 5c) revealed a well-coated surface of the carbon fibre with electrodeposited polymers. Energy-dispersive X-ray spectroscopy analysis confirmed the uniform distribution of the elements—namely, rhodium, nitrogen and fluorine—on the carbon fibre surface. Importantly, examination of the electrode surface after the ECD reactions demonstrated that the polymer coating remained intact, indicating its stability under the reaction conditions and aligning with our observation of successful recycling of the modified electrodes. Finally, cyclic voltammetry of **Rh-CME** was conducted under various scan rates (Fig. 5d). A good linear relationship was obtained from the graphs plotting the peak current (i_p) against the scan rate (υ), indicating that the rhodium catalysts have been successfully embedded on the electrode surface. Using an equation given in the literature[80,81], the surface rhodium catalyst loading for modified electrode was estimated to be 0.24 mol% for the ECD reactions at 0.2 mmol scale. Notably, if the reaction is further scaled up to a 2 mmol scale, the surface loading of the rhodium catalyst could be decreased to 0.05 mol% (Fig. 5e). This low catalyst loading further enhances the practicality and feasibility of our method. Analysis by inductively coupled plasma-mass spectrometry (ICP-MS) of a digested sample from the used **Rh-CME** electrode revealed a molar ratio of Rh/Ir exceeding 1,000:1, eliminating the possibility of metal exchange on the electrode surface (Supplementary Table 6).

Conclusion

In conclusion, we have demonstrated an electrocatalyst immobilization approach to realize the ECD reaction. A key insight from our study is that CME serves as a simple and effective solution to overcome the redox incompatibility issue, a problem that has seldom been addressed in organic electrosynthesis. This redox incompatibility originates from a strong correlation between hydricities of metal hydrides and reduction potential of parent metal complexes, which was validated experimentally. Furthermore, broad functional group tolerance and excellent chemoselectivity make this method particularly attractive for the stereochemical editing of bio-active compounds, especially those that prove difficult to access through asymmetric hydrogenation. Importantly, our strategy may extend beyond deracemization applications, providing a versatile approach for conducting incompatible reductions and oxidations within a single reaction vessel to achieve other elusive contra-thermodynamic transformations. In our ongoing work, we are further exploring the immobilization of chiral catalysts on both cathodes and anodes, with the aim of tackling more challenging deracemization reactions.

Methods

General procedure for ECD

Electrolysis was performed in an undivided cell with a carbon felt anode (10 mm × 30 mm × 3 mm) and a rhodium-catalyst-modified carbon felt cathode (**Rh-CME**, 10 mm × 30 mm × 3 mm). Under a nitrogen atmosphere, (*R,R*)-**Ir-1** (4.9 mg, 8 μmol, 4 mol%) and *rac*-**1** (0.20 mmol, 1 equiv.) were dissolved in 1,4-dioxane (2 ml) and aqueous KOH solution (11.2 mg, in 2 ml water). The reaction vessel was sealed and taken out of the glovebox. Eectrolysis was performed under a constant current of 1 mA for 24 h. The reaction was then quenched by saturated NH_4Cl solution (0.5 ml) and extracted by dichloromethane (5 ml × 3). The combined organic phase was dried over Na_2SO_4, concentrated in vacuo, and purified by flash column chromatography on silica gel to yield the desired product.

Data availability

The data supporting the findings of this study are available within the paper and its Supplementary Information, or from the authors on reasonable request. Crystallographic data for the structures reported in this Article have been deposited at the Cambridge Crystallographic Data Centre, under deposition nos. CCDC 2328338 ((*S*)-34). Copies of the data can be obtained free of charge at https://www.ccdc.cam.ac.uk/structures/. Source Data are provided with this paper.

References

1. Wang, P.-Z., Xiao, W.-J. & Chen, J.-R. Light-empowered contra-thermodynamic stereochemical editing. *Nat. Rev. Chem.* **7**, 35–50 (2022).
2. Huang, M., Pan, T., Jiang, X. & Luo, S. Catalytic deracemization reactions. *J. Am. Chem. Soc.* **145**, 10917–10929 (2023).
3. Blackmond, D. G. "If pigs could fly" chemistry: a tutorial on the principle of microscopic reversibility. *Angew. Chem. Int. Ed.* **48**, 2648–2654 (2009).
4. Chibata, I., Tosa, T. & Sano, R. Amino acid isomerization in the production of L-phenylalanine from D-phenylalanine by bacteria. *Appl. Microbiol.* **13**, 618–624 (1965).
5. Alexeeva, M., Enright, A., Dawson, M. J., Mahmoudian, M. & Turner, N. J. Deracemization of α-methylbenzylamine using an enzyme obtained by in vitro evolution. *Angew. Chem. Int. Ed.* **41**, 3177–3180 (2002).
6. Adair, G. R. A. & Williams, J. M. J. A novel ruthenium catalysed deracemisation of alcohols. *Chem. Commun*. 5578–5579 (2005).
7. Lackner, A. D., Samant, A. V. & Toste, F. D. Single-operation deracemization of 3H-indolines and tetrahydroquinolines enabled by phase separation. *J. Am. Chem. Soc.* **135**, 14090–14093 (2013).

8. Ji, Y., Shi, L., Chen, M. W., Feng, G. S. & Zhou, Y. G. Concise redox deracemization of secondary and tertiary amines with a tetrahydroisoquinoline core via a nonenzymatic process. *J. Am. Chem. Soc.* **137**, 10496–10499 (2015).
9. Wan, M., Sun, S., Li, Y. & Liu, L. Organocatalytic redox deracemization of cyclic benzylic ethers enabled by an acetal pool strategy. *Angew. Chem. Int. Ed.* **56**, 5116–5120 (2017).
10. Qu, P., Kuepfert, M., Jockusch, S. & Weck, M. Compartmentalized nanoreactors for one-pot redox-driven transformations. *ACS Catal.* **9**, 2701–2706 (2019).
11. Chen, F. et al. Simultaneous access to two enantio-enriched alcohols by a single Ru-catalyst: asymmetric hydrogen transfer from racemic alcohols to matching ketones. *ACS Catal.* **12**, 14429–14435 (2022).
12. Holzl-Hobmeier, A. et al. Catalytic deracemization of chiral allenes by sensitized excitation with visible light. *Nature* **564**, 240–243 (2018).
13. Troster, A., Bauer, A., Jandl, C. & Bach, T. Enantioselective visible-light-mediated formation of 3-cyclopropylquinolones by triplet-sensitized deracemization. *Angew. Chem. Int. Ed.* **58**, 3538–3541 (2019).
14. Li, X. et al. Photochemically induced ring opening of spirocyclopropyl oxindoles: evidence for a triplet 1,3-diradical intermediate and deracemization by a chiral sensitizer. *Angew. Chem. Int. Ed.* **59**, 21640–21647 (2020).
15. Plaza, M., Jandl, C. & Bach, T. Photochemical deracemization of allenes and subsequent chirality transfer. *Angew. Chem. Int. Ed.* **59**, 12785–12788 (2020).
16. Grosskopf, J. et al. Photochemical deracemization at sp^3-hybridized carbon centers via a reversible hydrogen atom transfer. *J. Am. Chem. Soc.* **143**, 21241–21245 (2021).
17. Plaza, M., Grosskopf, J., Breitenlechner, S., Bannwarth, C. & Bach, T. Photochemical deracemization of primary allene amides by triplet energy transfer: a combined synthetic and theoretical Study. *J. Am. Chem. Soc.* **143**, 11209–11217 (2021).
18. Kratz, T. et al. Photochemical deracemization of chiral alkenes via triplet energy transfer. *J. Am. Chem. Soc.* **144**, 10133–10138 (2022).
19. Kutta, R. J. et al. Multifaceted view on the mechanism of a photochemical deracemization reaction. *J. Am. Chem. Soc.* **145**, 2354–2363 (2023).
20. Shin, N. Y., Ryss, J. M., Zhang, X., Miller, S. J. & Knowles, R. R. Light-driven deracemization enabled by excited-state electron transfer. *Science* **366**, 364–369 (2019).
21. Zhang, C. et al. Catalytic α-deracemization of ketones enabled by photoredox deprotonation and enantioselective protonation. *J. Am. Chem. Soc.* **143**, 13393–13400 (2021).
22. Huang, M., Zhang, L., Pan, T. & Luo, S. Deracemization through photochemical *E*/*Z* isomerization of enamines. *Science* **375**, 869–874 (2022).
23. Onneken, C. et al. Light-enabled deracemization of cyclopropanes by Al-salen photocatalysis. *Nature* **621**, 753–759 (2023).
24. Wen, L. et al. Multiplicative enhancement of stereoenrichment by a single catalyst for deracemization of alcohols. *Science* **382**, 458–464 (2023).
25. Zhang, Z. & Hu, X. Visible-light-driven catalytic deracemization of secondary alcohols. *Angew. Chem. Int. Ed.* **60**, 22833–22838 (2021).
26. Gu, Z. et al. Deracemization through sequential photoredox-neutral and chiral Bronsted acid catalysis. *Angew. Chem. Int. Ed.* **61**, e202211241 (2022).
27. Wang, J., Peng, Y., Xu, J. & Wu, Q. Deracemization of racemic alcohols combining photooxidation and biocatalytic reduction. *Org. Biomol. Chem.* **20**, 7765–7769 (2022).
28. Wendlandt, A. E. Photocatalytic deracemization fixes the mix. *Science* **366**, 304–305 (2019).
29. Moeller, K. D. Synthetic applications of anodic electrochemistry. *Tetrahedron* **56**, 9527–9554 (2000).
30. Yan, M., Kawamata, Y. & Baran, P. S. Synthetic organic electrochemical methods since 2000: on the verge of a renaissance. *Chem. Rev.* **117**, 13230–13319 (2017).
31. Möhle, S. et al. Modern electrochemical aspects for the synthesis of value-added organic products. *Angew. Chem. Int. Ed.* **57**, 6018–6041 (2018).
32. Wiebe, A. et al. Electrifying organic synthesis. *Angew. Chem. Int. Ed.* **57**, 5594–5619 (2018).
33. Xiong, P. & Xu, H. C. Chemistry with electrochemically generated N-centered radicals. *Acc. Chem. Res.* **52**, 3339–3350 (2019).
34. Yuan, Y. & Lei, A. Electrochemical oxidative cross-coupling with hydrogen evolution reactions. *Acc. Chem. Res.* **52**, 3309–3324 (2019).
35. Jiao, K. J., Xing, Y. K., Yang, Q. L., Qiu, H. & Mei, T. S. Site-selective C–H functionalization via synergistic use of electrochemistry and transition metal catalysis. *Acc. Chem. Res.* **53**, 300–310 (2020).
36. Kingston, C. et al. A survival guide for the "electro-curious". *Acc. Chem. Res.* **53**, 72–83 (2020).
37. Liu, J., Lu, L., Wood, D. & Lin, S. New redox strategies in organic synthesis by means of electrochemistry and photochemistry. *ACS Cent. Sci.* **6**, 1317–1340 (2020).
38. Siu, J. C., Fu, N. & Lin, S. Catalyzing electrosynthesis: a homogeneous electrocatalytic approach to reaction discovery. *Acc. Chem. Res.* **53**, 547–560 (2020).
39. Wang, F. & Stahl, S. S. Electrochemical oxidation of organic molecules at lower overpotential: accessing broader functional group compatibility with electron–proton transfer mediators. *Acc. Chem. Res.* **53**, 561–574 (2020).
40. Novaes, L. F. T. et al. Electrocatalysis as an enabling technology for organic synthesis. *Chem. Soc. Rev.* **50**, 7941–8002 (2021).
41. Zhu, C., Ang, N. W. J., Meyer, T. H., Qiu, Y. & Ackermann, L. Organic electrochemistry: molecular syntheses with potential. *ACS Cent. Sci.* **7**, 415–431 (2021).
42. Malapit, C. A. et al. Advances on the merger of electrochemistry and transition metal catalysis for organic synthesis. *Chem. Rev.* **122**, 3180–3218 (2022).
43. Corma, A., Navas, J. & Sabater, M. J. Advances in one-pot synthesis through borrowing hydrogen catalysis. *Chem. Rev.* **118**, 1410–1459 (2018).
44. Reed-Berendt, B. G., Latham, D. E., Dambatta, M. B. & Morrill, L. C. Borrowing hydrogen for organic synthesis. *ACS Cent. Sci.* **7**, 570–585 (2021).
45. Santana, C. G. & Krische, M. J. From hydrogenation to transfer hydrogenation to hydrogen auto-transfer in enantioselective metal-catalyzed carbonyl reductive coupling: past, present, and future. *ACS Catal.* **11**, 5572–5585 (2021).
46. Zhang, Y., Lim, C.-S., Sim, D. S. B., Pan, H.-J. & Zhao, Y. Catalytic enantioselective amination of alcohols by the use of borrowing hydrogen methodology: cooperative catalysis by iridium and a chiral phosphoric acid. *Angew. Chem. Int. Ed.* **53**, 1399–1403 (2014).
47. Mutti, F. G., Knaus, T., Scrutton, N. S., Breuer, M. & Turner, N. J. Conversion of alcohols to enantiopure amines through dual-enzyme hydrogen-borrowing cascades. *Science* **349**, 1525–1529 (2015).
48. Rong, Z. Q., Zhang, Y., Chua, R. H., Pan, H. J. & Zhao, Y. Dynamic kinetic asymmetric amination of alcohols: from a mixture of four isomers to diastereo- and enantiopure α-branched amines. *J. Am. Chem. Soc.* **137**, 4944–4947 (2015).
49. Yang, P. et al. Nickel-catalyzed N-alkylation of acylhydrazines and arylamines using alcohols and enantioselective examples. *Angew. Chem. Int. Ed.* **56**, 14702–14706 (2017).

50. Xu, R. et al. Anti-Markovnikov hydroamination of racemic allylic alcohols to access chiral γ-amino alcohols. *Angew. Chem. Int. Ed.* **59**, 21959–21964 (2020).
51. Pan, H. J. et al. Catalytic diastereo- and enantioconvergent synthesis of vicinal diamines from diols through borrowing hydrogen. *Angew. Chem. Int. Ed.* **60**, 18599–18604 (2021).
52. Waldie, K. M., Ostericher, A. L., Reineke, M. H., Sasayama, A. F. & Kubiak, C. P. Hydricity of transition-metal hydrides: thermodynamic considerations for CO_2 reduction. *ACS Catal.* **8**, 1313–1324 (2018).
53. Hickey, D. P., Milton, R. D., Chen, D., Sigman, M. S. & Minteer, S. D. TEMPO-modified linear poly(ethylenimine) for immobilization-enhanced electrocatalytic oxidation of alcohols. *ACS Catal.* **5**, 5519–5524 (2015).
54. Das, A. & Stahl, S. S. Noncovalent immobilization of molecular electrocatalysts for chemical synthesis: efficient electrochemical alcohol oxidation with a pyrene–TEMPO conjugate. *Angew. Chem. Int. Ed.* **56**, 8892–8897 (2017).
55. Johnson, B. M., Francke, R., Little, R. D. & Berben, L. A. High turnover in electro-oxidation of alcohols and ethers with a glassy carbon-supported phenanthroimidazole mediator. *Chem. Sci.* **8**, 6493–6498 (2017).
56. Hashiguchi, S., Fujii, A., Takehara, J., Ikariya, T. & Noyori, R. Asymmetric transfer hydrogenation of aromatic ketones catalyzed by chiral ruthenium(II) complexes. *J. Am. Chem. Soc.* **117**, 7562–7563 (1995).
57. Hashiguchi, S. et al. Kinetic resolution of racemic secondary alcohols by Ru^{II}-catalyzed hydrogen transfer. *Angew. Chem. Int.* **36**, 288–290 (1997).
58. Nishibayashi, Y., Yamauchi, A., Onodera, G. & Uemura, S. Oxidative kinetic resolution of racemic alcohols catalyzed by chiral ferrocenyloxazolinylphosphine–ruthenium complexes. *J. Org. Chem.* **68**, 5875–5880 (2003).
59. Li, Y.-Y. et al. Kinetic resolution of racemic secondary alcohols catalyzed by chiral diaminodiphosphine–Ir(I) complexes. *Org. Lett.* **8**, 5565–5567 (2006).
60. Arita, S., Koike, T., Kayaki, Y. & Ikariya, T. Aerobic oxidative kinetic resolution of racemic secondary alcohols with chiral bifunctional amido complexes. *Angew. Chem. Int. Ed.* **47**, 2447–2449 (2008).
61. Galvin, C. M. & Waymouth, R. M. Electron-rich phenoxyl mediators improve thermodynamic performance of electrocatalytic alcohol oxidation with an iridium pincer complex. *J. Am. Chem. Soc.* **142**, 19368–19378 (2020).
62. Morris, R. H. Bronsted–Lowry acid strength of metal hydride and dihydrogen complexes. *Chem. Rev.* **116**, 8588–8654 (2016).
63. Murray, P. R. D. et al. Photochemical and electrochemical applications of proton-coupled electron transfer in organic synthesis. *Chem. Rev.* **122**, 2017–2291 (2022).
64. Deronzier, A. & Moutet, J. C. Functionalized polypyrroles. New molecular materials for electrocatalysis and related applications. *Acc. Chem. Res.* **22**, 249–255 (1989).
65. Chardon-Noblat, S., de Oliveira, I. M. F., Moutet, J.-C. & Tingry, S. Electrocatalytic hydrogenation on Poly$[Rh^{III}(L)_2(Cl)_2]^+$ (L=pyrrole-substituted 2,2′-bipyridine or 1,10-phenanthroline) films electrodes. *J. Mol. Catal. A* **99**, 13–21 (1995).
66. Heard, D. M. & Lennox, A. J. J. Electrode materials in modern organic electrochemistry. *Angew. Chem. Int. Ed.* **59**, 18866–18884 (2020).
67. Dieter, H., Sara, F., Iain, L. & Stefan, P. New Indanyloxyphenyl-cyclopropanecarb oxylic acids. Patent WO 2013/178575 A1 (27 May 2013).
68. Kennedy, S. H., Dherange, B. D., Berger, K. J. & Levin, M. D. Skeletal editing through direct nitrogen deletion of secondary amines. *Nature* **593**, 223–227 (2021).
69. Jurczyk, J. et al. Photomediated ring contraction of saturated heterocycles. *Science* **373**, 1004–1012 (2021).
70. Jurczyk, J. et al. Single-atom logic for heterocycle editing. *Nat. Synth.* **1**, 352–364 (2022).
71. Kern, J. C. et al. 1-Methyl-1H-pyrrole-2-carbonitrile containing tetrahydronaphthalene derivatives as non-steroidal progesterone receptor antagonists. *Bioorg. Med. Chem. Lett.* **20**, 4816–4818 (2010).
72. Ni, D. et al. Stereoselective [4+2]-cycloaddition with chiral alkenylboranes. *Angew. Chem. Int. Ed.* **59**, 11432–11439 (2020).
73. Lei, C., Yip, Y. J. & Zhou, J. S. Nickel-catalyzed direct synthesis of aryl olefins from ketones and organoboron reagents under neutral conditions. *J. Am. Chem. Soc.* **139**, 6086–6089 (2017).
74. Wang, Y., Carder, H. M. & Wendlandt, A. E. Synthesis of rare sugar isomers through site-selective epimerization. *Nature* **578**, 403–408 (2020).
75. Zhang, Y. A., Gu, X. & Wendlandt, A. E. A change from kinetic to thermodynamic control enables *trans*-selective stereochemical editing of vicinal diols. *J. Am. Chem. Soc.* **144**, 599–605 (2022).
76. Zhang, Y.-A. et al. Stereochemical editing logic powered by the epimerization of unactivated tertiary stereocenters. *Science* **378**, 383–390 (2022).
77. Oswood, C. J. & MacMillan, D. W. C. Selective isomerization via transient thermodynamic control: dynamic epimerization of *trans* to *cis* diols. *J. Am. Chem. Soc.* **144**, 93–98 (2022).
78. Castillo, C. E. et al. Electrochemical generation and spectroscopic characterization of the key rhodium(III) hydride intermediates of rhodium poly(bipyridyl) H_2-evolving catalysts. *Inorg. Chem.* **57**, 11225–11239 (2018).
79. Bakac, A. Aqueous rhodium(III) hydrides and mononuclear rhodium(II) complexes. *Dalton Trans* 1589–1596 (2006).
80. Bard, A. J. & Faulkner, L. R. *Electrochemical Methods: Fundamentals and Applications* (John wiley, 2001).
81. Wang, L. et al. Electrochemical driven water oxidation by molecular catalysts in situ polymerized on the surface of graphite carbon electrode. *Chem. Commun.* **51**, 7883–7886 (2015).

Acknowledgements

We are grateful for financial support from National Key R&D Program of China (grant no. 2022YFA1505100 to J.W.), the National Natural Science Foundation of China (grant no. 22201124 to J.W.), the Guangdong Provincial Key Laboratory of Catalysis (grant no. 2020B121201002 to J.W.) and the Innovation Commission of Shenzhen Municipality (grant no. 20231120100305001 to J.W.). We thank C. Huang for performing experiments during the paper's revision. We thank the Core Research Facilities for their assistance with performing ICP-MS, SEM and EDS experiments. The theoretical work was supported by the Center for Computational Science and Engineering at SUSTech. We thank X.-Y. Liu (Southern University of Science and Technology), G. Dong (University of Chicago) and Z. Huang (University of Hong Kong) for helpful discussions. We thank J. Gu (Southern University of Science and Technology) for assisting the EDS experiments.

Author contributions

J.W. conceived and designed the project. C.-J.Z. discovered the reaction and finished the optimization. C.-J.Z. and X.Y. performed other experiments. J.W. performed the computational work. J.W. and C.-J.Z. co-wrote the paper.

Competing interests

The authors declare no competing interests.

Additional information

Supplementary information The online version contains supplementary material available at https://doi.org/10.1038/s41929-024-01189-2.

Correspondence and requests for materials should be addressed to Jianchun Wang.

Peer review information *Nature Catalysis* thanks the anonymous reviewers for their contribution to the peer review of this work.